Fast Ignition Integrated Interconnecting Code (FI^3)
- Integrated Simulation and Element Physics -

H. Nagatomo 1), T. Johzaki 1), T. Nakamura 1), H. Sakagami 2), Y. Nakao 3), T. Taguchi 4), T., A. Sunahara 5), K. Nishihara 1), K. Mima 1)

1) Institute of Laser Engineering, Osaka University, Japan
2) National Institute for Fusion Science, Japan
3) Department of Applied Quantum Physics and Nuclear Engineering, Kyushu University, Japan
4) Department of Electrical and Electric Engineering, Setsunan University, Japan
5) Institute for Laser Technology, Japan

e-mail contact of main author: naga@ile.osaka-u.ac.jp

Abstract. The fast ignition (FI) scheme is one of the most fascinating and feasible ignition schemes for the inertial fusion energy. The numerical simulation plays an important role in studying detail mechanism of fast ignition, demonstrating the performance, designing the targets, and optimizing laser pulse shapes for the scheme. In order to study the physics of FI, we have developed "Fast Ignition Integrated Interconnecting code" (FI^3). In the result of the latest integrated simulation by FI^3, we find that density gap between cone tip and core plasma is important for the heating efficiency from hot electron to core plasma. We perform individual simulation of each element process also, and some important progresses are obtained. In the 2D simulation of laser plasma interaction by collective PIC code, we find that the electrons accelerated at the oblique inner surface of the cone cause three Maxwellian distributions in energy spectrum, which effects to the heating efficiency. About the formation of the high density fuel core plasma, we simulate the 2D non-spherical implosion using radiation hydrodynamic code. In result, we find non-spherical implosion is robust over hydrodynamic instability which is critical phenomena for spherical implosion. These two latest results are favorable facts for FI, and they will be reflected to the FI^3 simulation as feedback.

1. Introduction

The fast ignition (FI) scheme is one of the most fascinating and feasible ignition schemes for the inertial fusion energy (IFE) [1]. The numerical simulation and analysis play an important role in studying detail mechanism of fast ignition, demonstrating the performance, designing the targets and laser pulse shapes. In the previous IAEA/FEC, we have presented the feature of "Fast Ignition Integrated Interconnecting code" (FI^3) [2] and a representative numerical result. In FI^3, radiation hydrodynamic code, PINOCO [3] simulates implosion. Particle-in-Cell code, FISCOF [4] calculates relativistic laser plasma interaction. And relativistic Fokker-Planck hydrodynamic code, FIBMET simulates the hot electron transport and depositing electron energy in the core plasma as the meso-scale region [5].

Three element codes of which FI^3 consists are well sophisticated for the specific plasma conditions for each. Numerical analyses by the individual simulations are significant for understanding the physics of FI. In the following section 2, we present two important results. One is a radiation hydrodynamic simulation concerning the formation of high density fuel core plasma under the Rayleigh-Taylor instability using radiation hydrodynamic code. And next one is the generation of high energy electrons by the laser plasma interaction (LPI) inner surface of cone target. Finally, in section 3, a numerical result of fully integrated FI simulation is presented, where we have found that the scale length of pre-plasma in LPI is dominant factor for heating efficiency.

2. Element Codes and Their Physics

In the FI, imploded plasma reaches more than one thousand times of solid density, and relativistic hot electrons travel through the high density region with energy deposition, whereas phenomena under critical density is important for LPI. That is, very wide range in the density and time scale must be taken into account. In this situation, we have concluded that the most suitable way to simulate FI is connect three different code, PINOCO (radiation hydrodynamic code), FISCOF (collective PIC), and FIBMET (relativistic Fokker-Planck hydro code). At first, cone-guided implosion dynamics is calculated by PINOCO because radiation hydrodynamics is dominant in implosion process. At a shot timing of peta watt laser, the mass density, temperatures, and other profiles calculated by PINOCO are exported to both FISCOF and FIBMET for their initial and boundary conditions. The relativistic laser plasma interaction inside the cone target is simulated by collective PIC code, which exports the time-dependent energy distribution of fast electron to REP-hydro code. The fast electrons calculated by the FISCOF are exported to the FIBMET. Therefore, the core heating process is simulated using both physical profiles of imploded core plasma and fast electron as the boundary conditions. In this section, the features of the two computational codes, PINOCO and FISCOF are introduced with some latest calculated results.

2.1 Simulation of High Density Core Plasma in Non-spherical Implosion using PINOCO

The formation of high density core plasma is one of the most important issues for FI scheme, as well as heating core plasma problem. For the preliminary study, we have performed the non-spherical implosion with initial perturbation on the target surface to estimate the effect of RT instability. PINOCO which is 2D radiation hydro code is used where mass, momentum, electron energy, ion energy, equation of states, laser ray-trace, laser absorption, radiation transport, surface tracing and other related equations are solved simultaneously .

The cone with an opening angle of 30 degree is attached to a spherical shell of polystyrene (ρ=1.06 g/cm^3) which has a uniform thickness of 6 μm. The target is irradiated by uniform laser of which wavelength, energy and pulse width are, λ= 0.53 μm, 6.0 kJ and 1.2 ns (Gaussian, FWHM), respectively. About 70% of the total energy is used until they the maximum compression, that is, the effective laser energy is not more than 4.5kJ for each simulation. These target structure and laser pulse shape are not optimize for the cone-guided implosion, because the tailored pulse does not work well in some of them for the existence of the gold cone. If the spherical shell is irradiated by the low intensity laser, the ablated CH plasma hits the surface of the gold cone. That plasma blocks the irradiation of main laser pulse near the cone. For the limitation of computational resources, radiation transport is not included in all these simulations. The configuration of the target is shown in Fig. 4. For the comparison, some spherical implosions without cone target are also carried out. In these simulations, the initial perturbation of mode number ℓ= 0, 6, 12 and 24 are given onto the outer surface of CH ablator, and the amplitudes of the perturbation are 0, 0.1, 0.03, and 0.03 μm respectively. In the Table I, these simulation conditions are summarized. All the cases, the number of computational grid points is fixed to be 300x300 points, which are distributed to the shell target and gold cone region mainly.

Figure 2 shows the contours of the mass density and electron temperature at the timing of

maximum mass density of the case without initial perturbation (C-0) (Fig.2 (a)), and the case with perturbation of mode 24 (C-24) (Fig.2 (b)). Although the perturbation at the DT-CH interface is grown strongly due to the RT instability, they keep the almost same implosion velocity and obtained the maximum mass density at almost same timing. In both cases, the hot spot is pushed away from the center of implosion, and that dynamics enable to achieve the high averaged ρR. When the ρR is reached at the maximum, the tip of the gold cone still stay and keeps its shape, which is significant issue for the heating problem of fast ignition. The black lines indicate the contact surface between CH pusher and DT fuel. Around the cone, there are "dead area" where fuel are not accelerated, and not compressed sufficiently because of the existence of the cone. The open angle of the cone, cone material, and thickness of the cone will be optimizing parameters to control the implosion dynamics.

The calculated values of the maximum mass density and areal density ρR of the fuel at the maximum compression time is the essential for the fast ignition scheme. ρR and the maximum mass density are indicated in the table 1. Even though the maximum mass density of DT of case C-0 is lower than that of case S-0, the averaged ρR of case C-0 is higher than that of case S-0. This is caused by the shift of the hot spot and DT fuel drop into the center of the implosion. This fact was reported by our previous work [6] also. If there are initial perturbations, in the spherical implosion cases (S-6, 12 and 24), the averaged ρR are reduced to be 65% of the ideally spherical implosion case of S-0. On the other hand, in case C-6, 12, and 24, the averaged ρR are same level as the S-0 case, or higher. That is, non-spherical implosions are robust under the existence of non-linear hydrodynamic instabilities. In these simulations, the hydrodynamic instabilities of higher harmonic mode are appeared and grow rapidly, and they may affect to the results. For example, those implosions of S-6, 12 and 24 have similar attribute with each other. Even though the analysis of higher mode instability is important, we need more fine computational grids. Also, the radiation transport is not included in this work to save the computing time. The radiation transport may stabilize the RT instability, but the dynamics of the gold cone will be affected by the radiative heating also. Some our previous work suggests that the gold cone inside of the shell was ablated by the irradiation.

From these results, we concluded that even if there is hydrodynamic instability, high areal density can be achieved, though high temperature hot spot can not be expected which is required for conventional central ignition scheme. This is the advantage of fast ignition scheme.
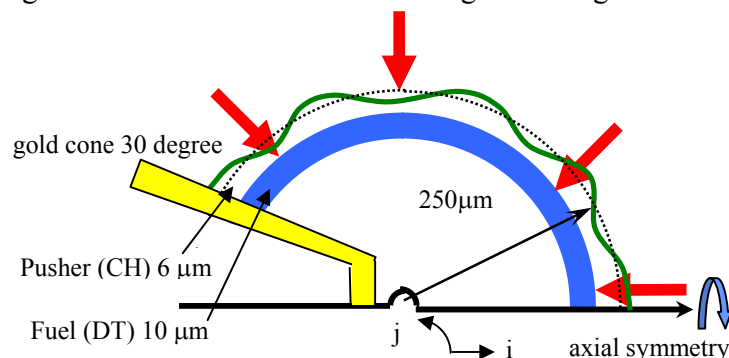
FIG.1. Target configuration for FIREX-I experiment, which is spherical CH-DT shell with gold conical target.
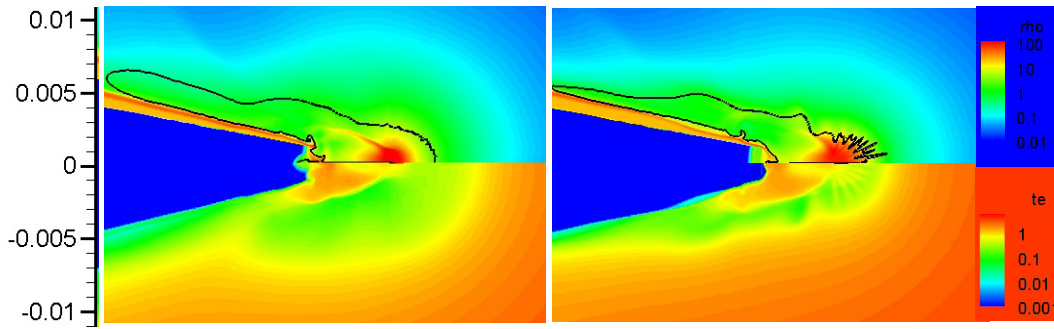
(a)   (b)

FIG. 2. Mass density contours in g/cm^3 (above) and electron temperature contours in keV (below), non-perturbed shell target (a) and a perturbed shell of mode $\ell =24$ (b). The black lines are contact surface between CH pusher and DT fuel.

TABLE I. Average ρR and fuel density.

	Spherical target				Cone-guided target			
perturbation mode	0	6	12	24	0	6	12	24
perturbation amplitude (μm)	(0)	0.10	0.03	0.03	(0)	0.10	0.03	0.03
case	S-0	S-6	S-12	S-24	C-0	C-6	C-12	C-24
averaged ρR (g/cm^2)	0.151	N/A	0.0981	0.0935	0.203	0.140	0.151	0.163
the maximum fuel density (g/cm^3)	250	N/A	163	145	133	89.0	101	104
averaged fuel density (g/cm^3)	137	N/A	83.7	77.8	93.1	64.9	69.3	72.2

2.2. Simulation of Laser Plasma Interaction of Cone Target by FISCOF-2D

One of the most significant progresses in these individual simulations is elucidation of generation of the high energy electrons in cone target. In the previous work, because of the limitation of computational resources, we could not treat two-dimensional simulation of high density plasma in cone target even though collective PIC was applied to save computational memory. Recently, two-dimensional large scale simulation is executed successfully [7]. For evaluation of fast electron generation due to relativistic laser-plasma interactions (LPI), we use the 1D or 2D collective PIC code (FISCOF-1D/2D) [7, 8], where collective particles are used to represent many normal particles and then total number of particles and computations are drastically reduced. Even though, the FISCOF-1D/2D code enables us to treat a wide range in space and high density region, the exact condition can not be considered for the limitation of computer resources. Therefore, FISCOF-1D is used when we simulate same scale size of plasma as the experiments. If geometric configuration must be taken into account in LPI simulation, FISCOF-2D is applied in a reduced region, and these fast electron beam profiles are extended to the practical scale size in FI^3.

Interaction of ultra-intense short pulse laser with cone target is studied using FISCOF-2D to understand the characteristics of high energy electrons emitted from the cone target and propagating towards core plasma for fast ignition [7]. Typical cone target geometry is shown in Fig.3. The density of cone target is 100 n_c with pre-plasma whose scale length is 1 micron. The target rear side is surrounded by underdense plasma whose density is 2 n_c which is taken from the result of hydro simulation (PINOCO). The initial electron temperature is set to 10 keV. Ion

motion is not taken into account which is considered acceptable for short laser pulse irradiation. The pulse has Gaussian profile in radial direction with focal spot size of 10 micron, and flat profile in time with duration of 150 fs, which irradiates the target from left boundary. The laser peak intensity is 5×10^{19} W/cm^2. Laser pulse is lowest mode of Hermite-Gauss mode, and is focused at the left boundary. Since the Rayleigh length is about 300 μm, most of the laser pulse reaches the target surface without diffraction. For the comparison, planner target with the same laser pulse as the cone target case is performed.
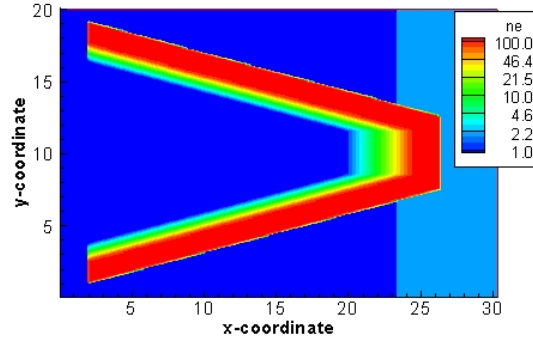
FIG. 3. The cone target geometry for 2D simulation (initial electron density profile).

The spectrums from cone and plane target are shown in fig. 4(a), and 4(b) respectively. It is found that there are three effective temperatures characterizing the hot electrons. For cone target case, the temperature for high energy component (T_h) is 5.0 MeV, and temperature for electrons of middle range (T_m) is 1.9 MeV. On the other hand, there are two temperatures in plane target. The temperature for high energy component is lower than T_h, and is down to 2.5 MeV. This temperature is explained with ponderomotive energy. The temperatures of low energy component are similar in both cases, but higher energy components are quite different. This is due to two important features of cone geometry, which are laser intensification by cone-guiding and larger interaction area at the cone wing. These two features lead to effective acceleration at cone tip and wing, which will be explained in the following subsections. The absorption rate is about 40 % for cone target, and 20 % for plane target. This higher coupling efficiency from laser to electrons is another advantage.

(a)   (b)
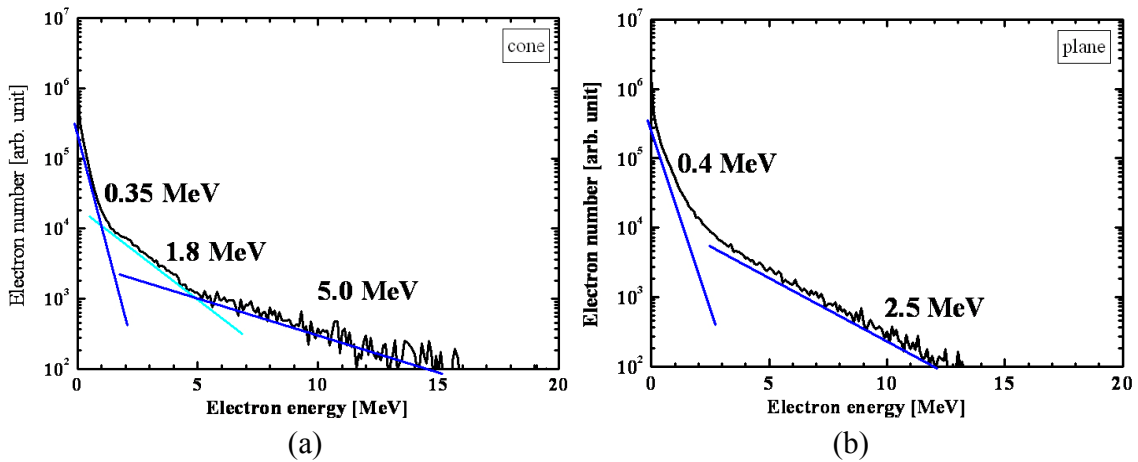
FIG. 4.   Electron spectrum of cone target (a) and electron spectrum of plane target (b) respectively.

2.3. Relativistic Fokker-Planck hydrodynamic code (FIBMET)

A 2-D Relativistic Fokker-Planck (RFP) code, FIBMET [5] has been applied for analysis of the fast electron transport and energy deposition processes in dense core plasma, which was coupled with an Eulerian hydrodynamic code to examine core-heating properties. In this code, cold bulk electrons and ions are treated by a 1-fluid and 2-temperature hydro model, and the fast electrons generated by the ignition laser-plasma interactions are treated by the RFP model. In the coupled RFP-hydro code includes magnetic field generated by fast electron current, gradient of plasma resistivity and pressure gradient. Initial and boundary condition of background plasma, injected electron beam can be imported from PINOCO and FISCOF-1D/2D. Numerical result of FIBMET is referred in following section

3. Fully Integrated Simulation of Fast Ignition

Using the time-dependent profiles of fast electron after passing through the low-density gap region, we carried out the core heating simulations using the 1D FP code. As for the bulk plasma profile, we use the imploded core profiles at the central axis ($r = 0$) obtained by r-z cylindrical 2D implosion simulation with PINOCO. The fast electrons are injected behind the cone tip (between the cone tip and the dense core). In fig.5 (a), spatial profiles of fast electron energy deposition at t = 2.5ps are plotted, in which we assume the scale length of LPI in FISCOF-1D is 1.0μm case. In the low-density region around the fast electron injection point, the Joule heating is comparable to the collisional heating due to the Coulomb interactions with bulk electrons. In the dense core region, the fast electron current can be easily cancelled by bulk electron flow with small drift velocity ($v_d << c$) because of much larger density of bulk electron than that of fast electron, so that the field effect is negligible and the collisional heating is dominant. The temporal evolution of ion and electron temperatures averaged over $\rho > 10\text{g/cm}^3$ region, $<T_k> = \int_{\rho>10\text{g/cm}^3} T_k(x) R_{DT}(x) dx \Big/ \int_{\rho>10\text{g/cm}^3} R_{DT}(x) dx$ where k denotes ion or electrons and $R_{DT}(x)$ is DT reaction rate at position x, are shown in Fig.5 (b) for the case of L_f = 1μm. Due to the collisional heating, the bulk electron is heated first, and then the bulk ion is heated via the temperature relaxation. Thus, the electron temperature reaches maximum ($<T_e>_{max}$=0.84keV) at t = 3.6ps, and then $<T_i>_{max}$ = 0.72 keV is obtained by 3 ps delay.

(a)   (b)
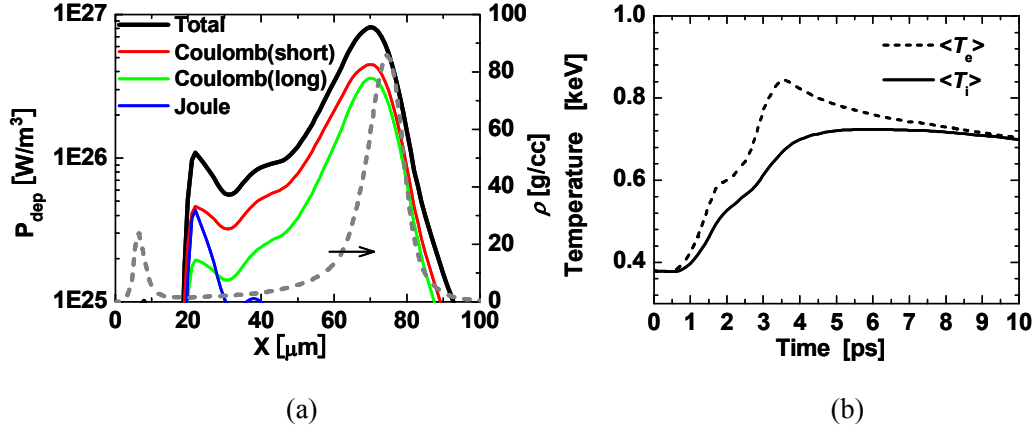
FIG. 5. Energy deposition profile of fast electron at t = 2.5ps for the case of L_f = 1μm (a). Temporal evolution of ion and electron temperature averaged over dense core region (ρ > 10g/cm³) in the case of L_f = 1μm (b).

The results of core heating simulations by varying L_f are summarized in fig.6 (a). Fig.6 (a) shows the scale length dependence of time-integrated energy of the fast electron beam (total and E < 2MeV component) and the energy deposited by fast electron inside the fuel plasma. The right axis indicates the energy coupling from laser to each value. In Fig.6 (b), the maximum value of $<T_i>$ is plotted as a function of L_f. With increasing L_f up to 1.5μm, the energy coupling from heating laser to fast electron becomes larger, so that the deposited energy and the resultant core temperature increase. The scale length becomes long furthermore, the total beam energy gradually decreases. However, the higher energy component (E > 2MeV) increases, so that the low energy component (E < 2MeV), which is effective in core heating, decreases faster than the total beam energy. As the result, the deposited energy in the fuel plasma and the resultant core temperature also decrease. These results indicate that the core heating efficiency depends not on the total beam energy but on the beam energy of low energy component (E <2MeV), *e.g.* in the case of L_f = 1μm, though the total beam energy is comparable to the case of L_f = 5μm, the beam energy of E < 2MeV component is 1.5 times as large, and then $<T_i>_{max}$ is higher by 0.17keV. In the present simulations, the optimum scale length for core heating is L_f = 1.5μm. In this case, the energy coupling from the heating laser to the core is 14.9% and ion in the core is heated up to 0.86keV (0.48keV rising). In the region of 1μm $\leq$ L_f $\leq$ 2μm, the heated core temperature is comparable to the value obtained at the experiments.

(a)   (b)
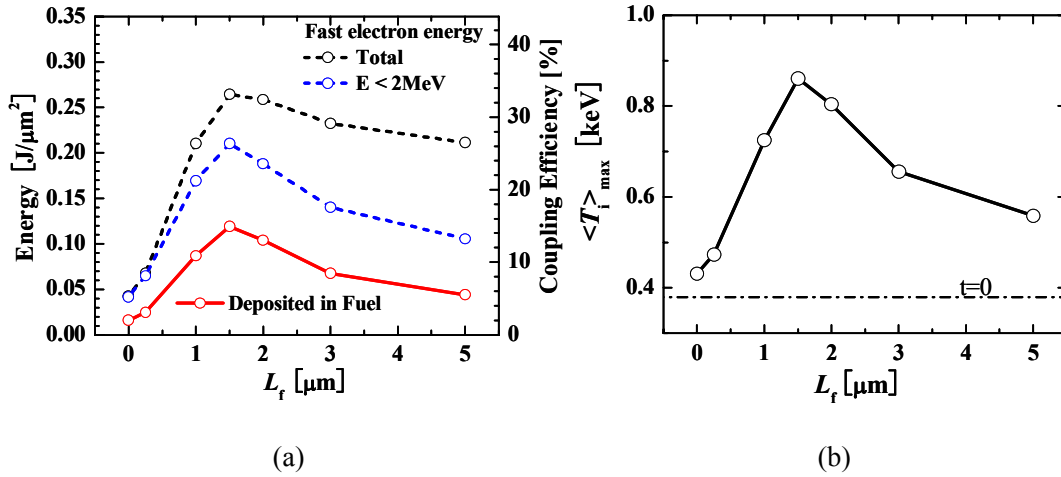
FIG. 6. Pre-plasma scale dependence of (a) total fast electron energy (black) and its E < 2MeV component (blue) and deposited energy of fast electron inside the fuel, and (b) maximum value of core ion temperature $<T_i>_{max}$.

4. Summary

Using FI^3 simulation system, integrated fast ignition simulation was performed. We have found that heating efficiency is very sensitive to the pre-plasma profile of the LPI which must be carefully controlled. Concerning the formation of high density fuel core plasma under the Rayleigh-Taylor instability, we have simulated the non-spherical implosion using radiation hydrodynamic code. Even though the fuel plasma was affected by the RT instability high areal density core plasma was achieved. In LPI simulation, we have found that there were three major mechanisms in accelerating the electrons, and a lot of effective hot electrons were generated on the inner surface of guiding cone.

With thus knowledge, we started up the design work for FIREX-I [9] project. We also recognized some improvements are required for the next step. For example, hybrid codes [10, 11] can simulate the filaments of relativistic electron beam in large scale which is important for electron energy transport.

Acknowledgement

References

[1] M. Tabak, et. al., Phys. Plasmas 1, 1626-1634, (1994).
[2] H.Nagatomo, et. al., IAEA-CN-116/IFP/07-29, (2004).
[3] H.Nagatomo, et. al., IAEA-CN-94/IFP/07, (2002).

[4] H. Sakagami, et al., J. Phys. IV Frances, **133**, 421-423, (2006).
[5] T. Johzaki, et al., J. Phys. IV Frances, **133**, 385-489, (2006).
[6] R. Kodama et. al., Nature 412 No.6849, 798-802 (2001).
[7] T. Nakamura, et al., J. Phys. IV Frances, **133**, 405-408, (2006).
[8] H. Sakagami, Proceedings of IFSA 2001, Paris: Elsevier, 434-437 (2003).
[9] Y. Izawa, et. al., IAEA-CN-116/OV/3-2, (2004).
[10] T. Taguchi, et al., Phys. Rev. Lett., **86**, 5055 (2001).
[11] T. Matsumoto, et al., Phys. of Plasmas, **13**, 052701, (2006).